

Supporting information

Wavelengths and lifetimes of paper autofluorescence: a simple substrate screening process to enhance the sensitivity of fluorescence-based assays in paper

Kamal G. Shah* and Paul Yager

Department of Bioengineering, University of Washington, Box 355061,
Seattle, Washington 98195, United States

* Email address: kgshah@uw.edu

Table of Contents

Supplementary Figure S1	S-2
Supplementary Figure S2	S-3
Application of the autofluorescence index to a paper-based nucleic acid amplification assay labeled with a low Stokes' shift fluorophore	S-4
<i>Motivation</i>	S-4
<i>Methods</i>	S-4
<i>Results and Discussion</i>	S-5
<i>References</i>	S-6

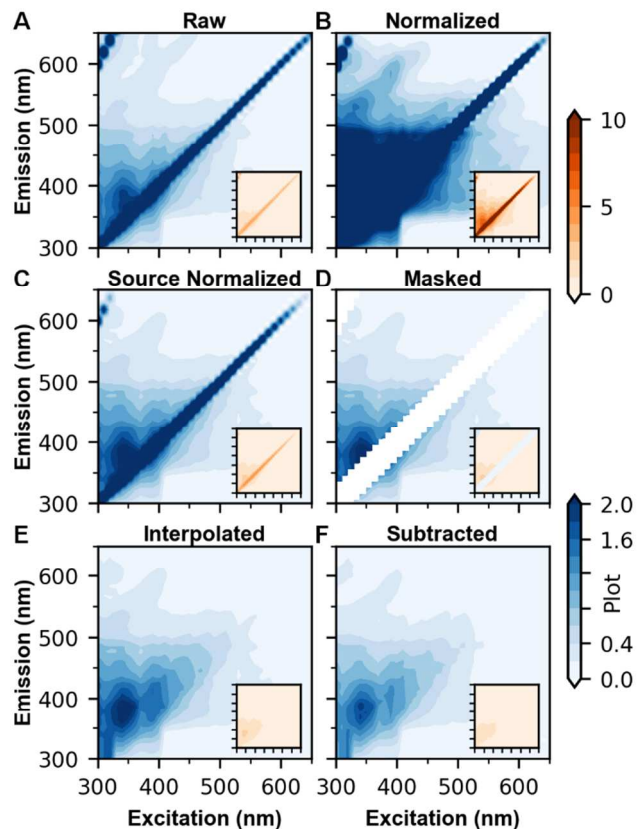


Figure S1: Summary of excitation-emission matrix (EEM) data processing for Millipore HF120 nitrocellulose. Z-axis shows fluorescence intensity at each excitation and emission wavelength pair. Insets show z-axis across a wider dynamic range. (a) Raw EEM as acquired by fluorimeter; (b) EEM normalized to photomultiplier tube spectral sensitivity; (c) EEM normalized by excitation source sensitivity; (d) EEM with first- and second-order Rayleigh scattering masked; (e) EEM with masked values linearly interpolated; and (f) EEM after subtracting that of a blank cuvette.

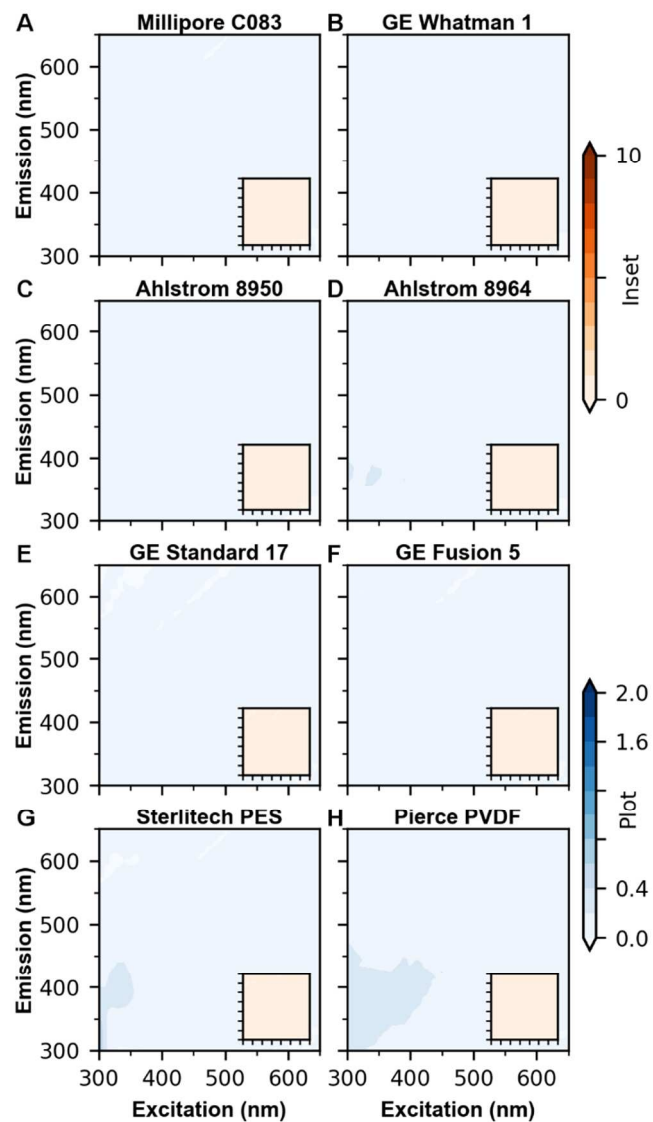


Figure S2: Excitation-emission matrices of several non-nitrocellulose paper membranes commonly used in paper microfluidics: (a) Millipore C083; (b) GE Whatman 1; (c) Ahlstrom 8950; (d) Ahlstrom 8964; (e) GE Standard 17; (f) GE Fusion 5; (g) Sterlitech Polyethersulfone; and (h) Pierce Polyvinylidene Difluoride. Z-axis shows fluorescence intensity at each excitation and emission wavelength pair. Insets show z-axis across a wider dynamic range.

Application of the autofluorescence index to a paper-based nucleic acid amplification assay labeled with a low Stokes' shift fluorophore

Note: Citations in the supporting information are independent of those in the manuscript itself.

Motivation

Many diagnostic assays rely on detecting pathogenic nucleic acids, including those for HIV and methicillin-resistant *Staphylococcus aureus* (MRSA).^{1,2} Isothermal nucleic acid amplification methods are a suitable alternative to polymerase chain reaction for the point of care due to their less stringent thermal and engineering constraints. Implementing such assays on paper substrates provides additional advantages by minimizing the thermal mass and cost of the system. Several such sample-to-result assays intended for the point of care have been demonstrated recently in the literature.^{2,3} The assay development process for point-of-care systems typically consists of selecting a suitable nucleic acid amplification biochemistry (e.g. loop-mediated amplification or strand-displacement amplification), identifying a suitable paper substrate (based on compatibility with the assay biochemistry and detection scheme),^{4,5} developing the necessary support hardware (including heaters, valves, and sample preparation), and optimizing the assay biochemistry to maximize performance; these steps typically last several months or years.

One critical component of assay development and optimization is choosing the paper substrate used to support the assay. Beyond compatibility with the nucleic acid amplification scheme, the substrate should also enable visualization of the assay output, typically with the use of an optical label. Our lab is in the process of converting our extant sample-to-result nucleic acid detection platform from colorimetric readout to fluorescence readout, which ought to reduce the complexity of the device and lower the time to result. As a first step toward developing this nucleic acid amplification fluorescence platform and rendering it suitable for the point of care, we have begun screening paper membranes to identify low-autofluorescence substrates. Here, we walk the reader through our screening methodology as it relates to demonstrating the application of the autofluorescence index.

Methods

Six membranes that have favorable fluidic (large volumetric capacity) and/or chemical compatibility with isothermal strand displacement amplification (iSDA) were identified (Ahlstrom 8950, Ahlstrom 8964, GE Standard 17, GE Fusion 5, GE Whatman 1, and Millipore C083). Nitrocellulose membranes were not considered as they were determined previously to be poor substrates for iSDA.⁶ Membranes were cut to 2 cm diameter circles using a mechanical punch and placed in individual wells of a 12-well plate. Rather than optimize the nucleic acid amplification assay biochemistry on each membrane (which could take several weeks per membrane due to the need to titrate each reagent), we first used the autofluorescence index to rapidly screen membranes based on the ability to visualize the fluorescence output of a successful iSDA run.

AquaPhluor-593 (a Texas Red analog) was used as part of a Pleiades probe (with a minor groove binder) to label the output of iSDA. Its peak excitation (593 nm) and emission (615 nm) wavelengths correspond to a window of low autofluorescence for the identified papers based on Figure S2. Moreover, AquaPhluor-593 (AP-593) has a relatively constant fluorescence emission across a wide range of pH and temperatures (unlike Texas Red or AlexaFluor 594) and is suitable for detection with a point-of-care instrument such as a mobile phone (as are Texas Red and AlexaFluor 594). Reaction mixes were prepared by mixing K_2PO_4 (500 mM, 60 μL), MgSO_4 (100 mM,

22.5 μL), dNTPs (10 mM, 12 μL), trehalose (37%, 1M, 162 μL), 500 kD dextran (72 μL), *ldh1* primers (500 nM forward, 250 nM reverse, 50 nM each bumper, 30 μL , ELITechGroup; sequences previously reported),² *ldh1* fluorescent probe (4 μM , 30 μL ; 5'-AP-593-CTA ATT CAT CAA CAA TGC-minor groove binder nonfluorescent quencher-3', ELITechGroup), nuclease-free water (127.2 μL), WarmStart Bst polymerase (8000 U/ μL , 15 μL , New England Biolabs), and Nt.BbvC1 nicking enzyme (0.2 U/ μL , 9.6 μL , mutant strain, New England Biolabs). Reaction tubes were prepared by adding either MRSA genomic DNA (10^4 copies/ μL , 6 μL , ATCC) or nuclease-free water (6 μL) and 54 μL of reaction mix. Three positive and three negative reaction tubes were prepared. iSDA was performed by incubating each tube at 49 °C for 60 minutes. The output of each reaction tube (10 μL) was pipetted onto each membrane and imaged while each membrane was still wet. The detector used was a mobile phone (LG Nexus 5X) with a Texas red excitation and emission filter (Semrock) on the cell phone flash and camera, respectively. Images were acquired at ¼ second exposure and ISO 6400; spot intensities were quantified in ImageJ. Gamma-corrected mean spot intensities of the red channel were compared between membranes; for each membrane type, spots were considered positive if they were greater than the mean plus 2.92 times the standard deviation of the negative control spots (threshold based on *t*-statistics for $\alpha=5\%$ and 2 degrees of freedom).

Results and Discussion

Figure S3 below shows representative photos of iSDA endpoint fluorescence on paper. On each membrane, three (of three) distinct spots are visually observable for those corresponding to MRSA gDNA-positive reaction tubes, whereas zero spots (of three) are visually observable for those corresponding to MRSA-negative tubes. Images were acquired at the highest exposure and sensitivity (1/4 second and ISO 6400, respectively) possible for the Nexus 5X to maximize photon capture.

Table S1 indicates the mean and standard deviation of spots corresponding to MRSA gDNA-positive and MRSA gDNA-negative tubes, along with the statistical thresholds for a positive result and fraction of spots greater than this criterion. All spots corresponding to MRSA gDNA-positive tubes were above the threshold for positive spots except on Millipore C083, the membrane with the highest autofluorescence index, for which only one of three spots was above the threshold. Indeed, Millipore C083 had the greatest autofluorescence index, spot intensities, and threshold for positive of all materials evaluated.

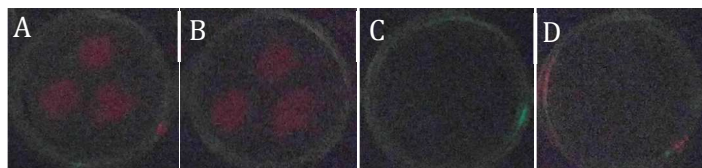


Figure S3: Representative photos of iSDA endpoint fluorescence (images are not gamma-corrected). iSDA was performed in-tube and the output was spotted onto porous membranes: (a) Ahlstrom 8950 (MRSA gDNA-positive); (b) Ahlstrom 8964 (MRSA gDNA-positive); (c) Ahlstrom 8950 (MRSA gDNA-negative); and (d) Ahlstrom 8964 (MRSA gDNA-negative). Three spots are visible on each membrane corresponding to tubes that were MRSA gDNA-positive (a and b), whereas no spots are visible for spots corresponding to tubes that were MRSA gDNA-negative (c and d).

The threshold for positive was much greater on Millipore C083 than on the other membranes because of the greater intensity of the negative spot and slightly greater coefficient of variation. Indeed, the negative spot intensity was greater on Millipore C083 than on each of the other materials ($p < 0.01$, Welch's t -test). Based on these data, we eliminated Millipore C083 from consideration as a substrate to support iSDA in paper. Rather, we have been exploring GE Fusion 5, GE Standard 17, and Ahlstrom 8950 due to their low autofluorescence (as indicated by both low negative spot intensities and low autofluorescence indices) and favorable fluidic and chemical compatibility with iSDA.

Use of the autofluorescence index in substrate screening is advantageous because it enables rationally (rather than arbitrarily) identifying potential paper membranes. The autofluorescence index reduces the need to optimize an assay on several potential paper substrates, which is time-consuming and costly (requiring weeks or months of experiments in our experience as all 12 assay reagents must be titrated independently). This is because the autofluorescence index provides a metric that corresponds to the expected signal observed in an assay based on the spectral overlap between a fluorophore's spectral emission and that of paper autofluorescence, while also accounting for the detector's spectral sensitivity. In our case, use of the autofluorescence index to screen membranes would have eliminated Millipore C083 from consideration (thereby eliminating the need to validate iSDA on Millipore C083).

Table S1: Autofluorescence index and iSDA spot intensities on several paper substrates

	Autofluorescence index	Negative spot intensity[†]	Positive spot intensity[†]	Threshold for positive[†]	Fraction above threshold
Ahlstrom 8950	1500	5.5 ± 0.69	21 ± 2.9	8	3/3
Ahlstrom 8964	1720	7.7 ± 0.19	39 ± 1.3	8	3/3
GE Standard 17	1090	11 ± 2	20 ± 2.3	16	3/3
GE Fusion 5	924	9 ± 0.88	18 ± 1	12	3/3
GE Whatman 1	1610	12 ± 1.6	19 ± 1.8	16	3/3
Millipore C083	2850	47 ± 9	74 ± 5.6	73	1/3

†: Mean and standard deviation of the gamma-corrected red color channel intensities are tabulated.

References cited in supporting information

Note: Citations in the supporting information are independent of those in the manuscript itself.

- (1) Rohrman, B. A.; Leautaud, V.; Molyneux, E.; Richards-Kortum, R. R. *PLoS One* **2012**, *7* (9), e45611.
- (2) Lafleur, L.; Bishop, J. D.; Heiniger, E. K.; Gallagher, R. P.; Wheeler, M. D.; Kauffman, P. C.; Zhang, X.; Kline, E.; Buser, J.; Ramachandran, S.; Byrnes, S.; Vermeulen, N.; Scarr, N.; Belousov, Y.; Mahoney, W.; Toley, B. J.; Ladd, P. D.; Lutz, B.; Yager, P. *Lab Chip* **2016**, *52* (19), 3377–3383.
- (3) Tang, R.; Yang, H.; Gong, Y.; You, M.; Liu, Z.; Choi, J. R.; Wen, T.; Qu, Z.; Mei, Q.; Xu, F. *Lab Chip* **2017**, *17* (7), 1270–1279.
- (4) Linnes, J. C.; Rodriguez, N. M.; Liu, L.; Klapperich, C. M. *Biomed. Microdevices* **2016**, *18* (2), 1–12.
- (5) Anderson, C. E.; Shah, K. G.; Yager, P. In *Methods in Enzymology*.
- (6) Monahan, C. M. Fluorescence Detection of DNA Amplification in Porous Media for Point-of-Care Diagnostics, University of Washington, 2015.